Efficient ultimate load estimation for offshore wind turbines using interpolating surrogate models

Van Den Bos, L. M.M.; Sanderse, B.; Blonk, L.; Bierbooms, W. A.A.M.; Van Bussel, G. J.W.

DOI
10.1088/1742-6596/1037/6/062017

Publication date
2018

Document Version
Final published version

Published in
Journal of Physics: Conference Series

Efficient ultimate load estimation for offshore wind turbines using interpolating surrogate models

IOP Conf. Series: Journal of Physics: Conf. Series **1037** (2018) 062017 doi:10.1088/1742-6596/1037/6/062017

Efficient ultimate load estimation for offshore wind turbines using interpolating surrogate models

L M M van den Bos[1,2], B Sanderse[1], L Blonk[3], W A A M Bierbooms[2] and G J W van Bussel[2]

[1] Centrum Wiskunde & Informatica, P.O. Box 94079, 1090 GB, Amsterdam, the Netherlands
[2] Delft University of Technology, P.O. Box 5, 2600 AA, Delft, the Netherlands
[3] DNV GL, P.O. Box 2029, 9704 CA, Groningen, the Netherlands

E-mail: l.m.m.van.den.bos@cwi.nl

Abstract. During the design phase of an offshore wind turbine, it is required to assess the impact of loads on the turbine life time. Due to the varying environmental conditions, the effect of various uncertain parameters has to be studied to provide meaningful conclusions. Incorporating such uncertain parameters in this regard is often done by applying binning, where the probability density function under consideration is binned and in each bin random simulations are run to estimate the loads. A different methodology for quantifying uncertainties proposed in this work is polynomial interpolation, a more efficient technique that allows to more accurately predict the loads on the turbine for specific load cases. This efficiency is demonstrated by applying the technique to a power production test problem and to IEC Design Load Case 1.1, where the ultimate loads are determined using BLADED. The results show that the interpolating polynomial is capable of representing the load model. Our proposed surrogate modeling approach therefore has the potential to significantly speed up the design and analysis of offshore wind turbines by reducing the time required for load case assessment.

1. Introduction

It is required to assess various load cases during the design phase of a wind turbine. The IEC standard for offshore wind turbines [1] prescribes several load cases that should be modeled, varying from fatigue analysis in calm sea to ultimate load cases. Due to the uncertain environmental conditions, the wind and sea conditions have to be modeled stochastically according to a prescribed distribution.

To determine the influence of uncertain parameters, it is customary to first divide the ranges of the distributions under consideration in bins, subsequently to randomly draw samples in each bin (the so-called seeds), and finally to accumulate the results. This is suggested in the aforementioned standard [1] and commonly applied in literature (e.g. [2, 3, 4, 5]). In case of uncertain (mean) wind speed, often the bins are chosen independently from the distribution under consideration and solely depend on the cut-in and cut-out speed of the wind turbine.

The challenge of such calculations is the computational effort that is necessary to evaluate a wind turbine model several times to assess the loads for various environmental conditions. Several more efficient methods exist to characterize the influence of uncertainties on a quantity of interest [6]. One class of commonly applied efficient methods is formed by polynomial surrogate models. The key idea is to replace the computationally expensive computer model with a polynomial

that approximates the true model, but can be evaluated very fast. Initial applications of such methods already exist in wind energy literature [7], for example based on polynomial surrogates in combination with binning [8, 9, 10], proper orthogonal decompositions [11], or more efficient Monte Carlo sampling methods [12, 13]. In this article, we propose the use of interpolation using a nested sequence of nodes, called Leja nodes. This approach has the benefits that the full distribution is taken into account (i.e. binning is not necessary anymore) and that it is accompanied with strong mathematical proofs of its exactness (i.e. the surrogate model approximates the computationally expensive model very well). Moreover the sequence is nested, such that refining the surrogate can be done by adding new model evaluations and reusing all existing ones.

The test problem under consideration is based on Design Load Case (DLC) 1.1 [1], that describes the calculation of ultimate loads of a wind turbine operating under normal conditions. The offshore wind turbine under consideration is the NREL 5MW turbine [14].

This article is set up as follows. In Section 2 the procedure to construct a surrogate is discussed. To demonstrate the methodology, the procedure is applied to a simple power production test problem in Section 3. Section 4 contains the results of applying this methodology to DLC 1.1. In Section 5 the article is concluded and options for future research are discussed.

2. Interpolation using Leja nodes

The goal is to replace a computationally expensive computer model with an efficient polynomial. This is done through interpolation: the model is evaluated at several a-priori chosen locations and a polynomial is constructed that matches the value of the model at these locations. The construction of such a polynomial is discussed in Section 2.1 and the algorithm to select the nodes is discussed in Section 2.2.

2.1. Polynomial interpolation

The key problem is as follows. The wind turbine computer model is modeled mathematically as a function $u : \Omega \to \mathbb{R}$, i.e. evaluating u yields ultimate loads on the turbine given parameters from the set Ω (such as the sea state and wind speed). The goal is to approximate the statistical properties of $y = u(x)$, where x has distribution ρ. This can be seen as determining the effect of the environmental conditions (modeled with ρ) on the loads (modeled by y). For example, the mean of y can be denoted explicitly as follows:

$$\mathbb{E}[y] = \mathbb{E}[u(x)] = \int_\Omega u(x)\,\rho(x)\,\mathrm{d}x. \tag{2.1}$$

As stated previously, it is common to approximate this integral by binning Ω and approximating the integrals on the bins with random samples. In contrast, we choose to approximate u directly and for this purpose an interpolating polynomial is constructed. To this end, let $\{x_0, \ldots, x_N\} \subset \Omega$ be $N+1$ nodes, which can be seen as samples of the distribution ρ. The interpolant (say $\hat{u}_N$) can be constructed explicitly by enforcing that it is a polynomial of degree N and is exact in the nodes, i.e. $\hat{u}_N(x_k) = u(x_k)$. After constructing the interpolating polynomial, the mean and other statistical properties can be determined efficiently using straightforward methods found in literature (such as Monte Carlo), or even analytically if the statistical moments of the input distributions are known.

For a single parameter, i.e. $\Omega = \mathbb{R}$, the interpolating polynomial can be constructed as follows. Let $L_k(x)$ (for $k = 0, \ldots, N$) be the Lagrange basis polynomials, defined as follows (cf. [15]):

$$L_k(x) = \prod_{\substack{j=0 \\ j \neq k}}^{N} \frac{x - x_j}{x_k - x_j}. \tag{2.2}$$

These polynomials have the property that $L_k(x_j) = 1$ if $j = k$ and $L_k(x_j) = 0$ otherwise. The interpolating polynomial can then be constructed as follows:

$$\hat{u}_N(x) = \sum_{k=0}^{N} L_k(x) u(x_k). \tag{2.3}$$

This construction in combination with the definition of the Lagrange basis polynomials yields $\hat{u}_N(x_k) = u(x_k)$ for all k.

The construction can be generalized to the multivariate case as follows. Let the Vandermonde-matrix be given as follows:

$$V(X_N) = \begin{pmatrix} \varphi_0(x_0) & \cdots & \varphi_0(x_N) \\ \vdots & \ddots & \vdots \\ \varphi_N(x_0) & \cdots & \varphi_N(x_N) \end{pmatrix}, \tag{2.4}$$

where $\varphi_0, \ldots, \varphi_N$ are N independent multivariate polynomials. This matrix has the property that $\det V(X_N) = 0$ if two nodes coincide, so it can be used to generalize the definition of L_k as follows:

$$L_k(x) = \frac{\det V_k(X_N)}{\det V(X_N)}, \tag{2.5}$$

where $V_k(X_N)$ equals $V(X_N)$ where x_k is replaced by x. The Lagrange interpolating polynomial can now be constructed in exactly the same way as in the univariate case.

2.2. Leja nodes

The interpolation error, i.e. the difference between the interpolant $\hat{u}_N$ and the model u, scales for a given x with $\prod_{j=0}^{k} |x - x_j|$. From this idea, the Leja nodes emerge, which are defined by determining the location where this error is maximal (cf. [16]). A probability density function (PDF) can be incorporated as scaling parameter, such that the definition becomes:

$$x_{k+1} = \arg\max_{x \in \Omega} \left((\rho(x) + \zeta) \prod_{j=0}^{k} |x - x_j| \right). \tag{2.6}$$

Here $\zeta \geq 0$ is a tempering parameter that can be used to create a more predictable and stable interpolation sequence [17]. These nodes depend on the distribution under consideration and the next one is determined using all the previous ones, so it is possible to assess the accuracy of the current interpolant and only refine it if necessary.

The role of ζ can be characterized as follows. Let $\rho_\zeta(x) \propto \rho(x) + \zeta$, with $\int_\Omega \rho_\zeta(x)\,\mathrm{d}x = 1$, i.e. ρ_ζ is a PDF. Then $\rho_\zeta(x) \propto \vartheta\rho(x) + (1 - \vartheta)$, with $\vartheta = 1/(\zeta + 1)$. A larger ζ reduces the effect of ρ and moves ρ_ζ to a uniform distribution. The "best" value of ζ depends on the regularity of the model and the distribution under consideration and is chosen heuristically in this article.

In the univariate case, Leja nodes can be determined efficiently by solving the maximization problem (2.6) directly. In multivariate cases, this maximization problem is difficult to solve straightforwardly, so we resolve to randomly sampling the space and selecting the node that maximizes the target function. The resulting Leja sequences for the bivariate standard Gaussian distribution are depicted in Figure 1. It is clearly visible that by choosing a higher ζ (chosen arbitrarily here), the nodes are more spread out across the space.

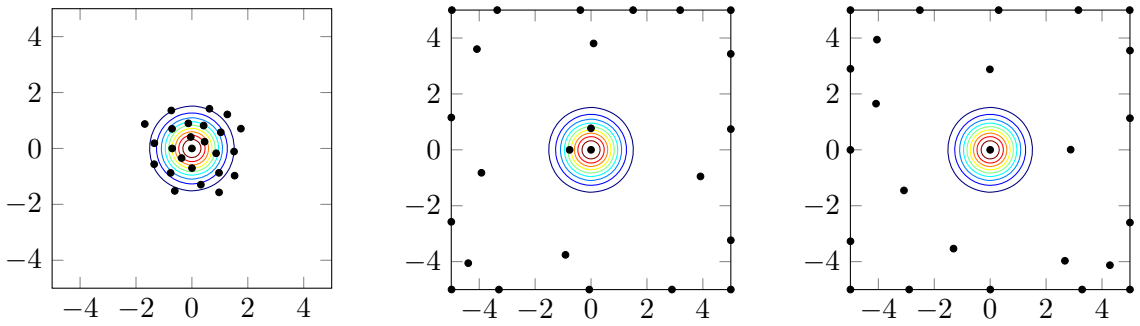

(a) $\zeta = 0$ **(b)** $\zeta = 1/10$ **(c)** $\zeta = 1$

Figure 1: Two dimensional Leja nodes with respect to the bivariate standard normal distribution.

3. Power Production example

Although the key focus in this article is on load calculation, it is instructive to discuss a relatively straightforward power production example to demonstrate the methodology and visualize advantages and disadvantages of the approach. The example discussed in this section is a basic power production example, where the uncertainty under consideration is an uncertain 10-minute wind speed average and the model under consideration is a scaled P-v curve that maps 10-minute wind speed averages to power production.

To this end, let the P-v curve (denoted as $u(v)$ to overcome confusion with probability) be defined as follows:

$$u(v) = \begin{cases} 0 & \text{if } v \leq v_{\text{cutin}}, \\ \left(\frac{v - v_{\text{cutin}}}{v_{\text{rated}} - v_{\text{cutin}}}\right)^3 & \text{if } v_{\text{cutin}} < v \leq v_{\text{rated}}, \\ 1 & \text{if } v_{\text{rated}} < v \leq v_{\text{cutout}}, \\ 0 & \text{if } v_{\text{cutout}} < v. \end{cases} \tag{3.1}$$

The distribution of v under consideration is a Weibull distribution, parametrized by two parameters: a scale parameter λ and a shape parameter k. Both have to be positive. The PDF of v then equals:

$$\rho(v) = \begin{cases} \frac{k}{\lambda}\left(\frac{v}{\lambda}\right)^{k-1} \exp\left[-\left(\frac{v}{\lambda}\right)^k\right] & \text{if } v > 0, \\ 0 & \text{otherwise.} \end{cases} \tag{3.2}$$

For the purpose of this test case, the parameters are chosen according to the following list.

v_{cutin}	v_{rated}	v_{cutout}	λ	k
3 m/s	10 m/s	25 m/s	10 m/s	2

The resulting distribution and P-v curve are depicted in Figure 2. Using $\zeta = 0$ and $\zeta = 1/3$, the model $u(v)$ can be interpolated using Leja nodes (defined by (2.6)), see Figure 3. The distribution of $u(v)$ determined with these ζ is also depicted in Figure 3 (using a kernel density estimate), and it can clearly be observed that the approximation for $\zeta = 1/3$ is indeed better.

Note that this model is only piecewise differentiable: there is a jump in the derivative at $v = v_{\text{rated}}$. It can be observed that the Leja nodes are constructed such that the accuracy is high with respect to the distribution. For $\zeta = 0$, the interpolation is therefore accurate near

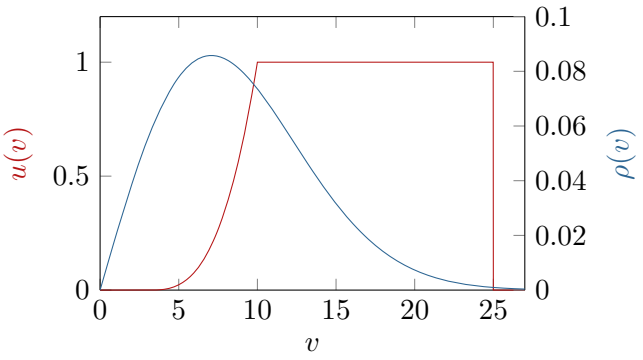

	$\mathbb{E}[u]$	$\sigma[u]$
Exact	5.06×10^{-1}	4.34×10^{-1}
$\zeta = 0$	5.16×10^{-1}	4.47×10^{-1}
$\zeta = 1/3$	5.15×10^{-1}	4.45×10^{-1}

Figure 2 & Table 1: The P-v curve (in red) and the distribution (in blue) under consideration for the propagation problem. The exact mean and standard deviation of this problem are listed in the table.

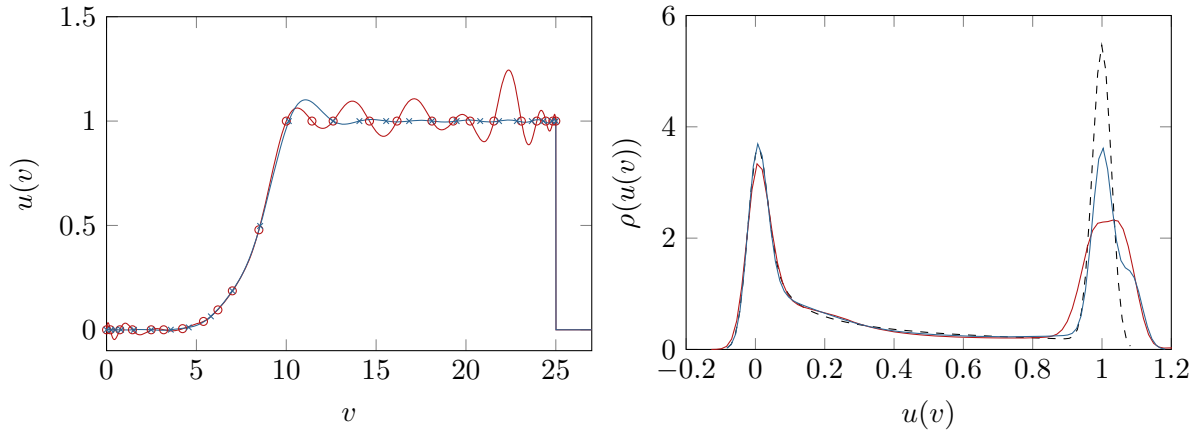

Figure 3: The interpolated P-v curve and the resulting distribution of $u(v)$ using 25 nodes (shown in the left figure) for the propagation problem with $\zeta = 0$ (in red) and $\zeta = 1/3$. (in blue). The dashed distribution is the exact distribution.

$v = 5$, which is the region of high probability. However, the accuracy deteriorates significantly in regions with low probability, which is often not wanted. It is clear that the tempering parameter ζ reduces this effect significantly and yields a more global accurate result at the cost of slightly less accuracy in the region with high probability. This effect is even stronger in the output PDF, where $\zeta = 0$ yields a significantly larger error at $v = v_{\text{rated}}$ than $\zeta = 1/3$.

Although the number of nodes is relatively small, the mean and standard deviation can be determined with decent accuracy, see Table 1. Both values of ζ show similar results.

Binning and Monte Carlo approaches are randomized approaches, so a straightforward comparison of the mean and standard deviation cannot be made. However, at least 5 seeds per bin (resulting into 110 evaluations) are necessary to reach a similar accuracy, where the bins have size 1 m/s. To reach a similar accuracy with a Monte Carlo approach, at least 10^3 samples are required. Here, accuracy is measured using the standard deviation of consecutive runs, such that still a large number of runs with these number of nodes produces a larger error. This confirms the well-known fact that, given sufficiently smooth functions, interpolation approaches converge

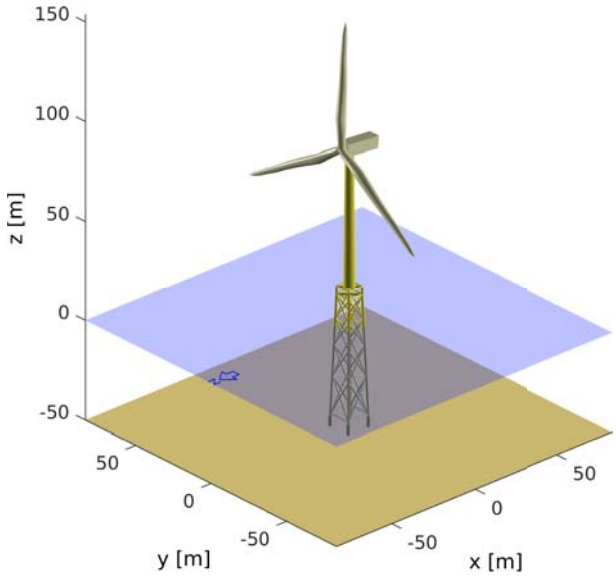

Figure 4: Sketch of the geometry of the NREL 5MW Offshore Wind turbine.

faster than random sampling approaches [6].

4. Design Load Case 1.1 applied to the NREL 5MW Baseline Wind turbine

Design Load Case (DLC) 1.1 encompasses assessing the effect of normal wind and sea conditions during normal power production on the ultimate loads of the turbine. For offshore wind turbines, it is compulsory to use representative mean wind and sea states, although a so-called normal turbulence model (NTM) and a normal sea state (NSS) can be assumed [1, 18].

The proposed methodology in this article is applied to the NREL 5MW wind turbine [14], see Figure 4 for a sketch. The goal of this article is not to assess the loads of the NREL 5MW in great detail, but to discuss the applicability of the proposed interpolation procedure to a case where the IEC standard is followed as much as possible. To this end, the extrapolation step (which is essentially the purpose of DLC 1.1) is omitted, as it requires further analysis before it can be carried over in the mathematical framework set out in this article.

The ultimate loads of the offshore wind turbine under consideration are determined using BLADED 4.6. Before diving into the results, the wind and sea conditions are discussed in Section 4.1 and 4.2. The uncertain parameters are summarized in Table 2. The results of the procedure are discussed in Section 4.3.

4.1. Wind conditions

The wind turbine class under consideration is $\mathrm{I_A}$, which is the class with the highest reference wind speed $V_{\mathrm{ref}} = 50\,\mathrm{m/s}$ and highest turbulence characteristics resulting into the highest reference mean turbulence intensity over a 10 minute period of time, $I_{\mathrm{ref}} = 0.16$. The annual average wind speed, V_{ave}, then becomes $V_{\mathrm{ave}} = 0.2V_{\mathrm{ref}} = 10\,\mathrm{m/s}$.

The mean wind speed at hub height over a 10 minute period of time, V_{hub}, is assumed to follow a Rayleigh distribution given by:

$$\rho(V_{\mathrm{hub}}) = \frac{V_{\mathrm{hub}}}{\sigma_V^2} \exp\left[-\frac{V_{\mathrm{hub}}^2}{2\sigma_V^2}\right], \tag{4.1}$$

with $\sigma_V = V_{\mathrm{ave}}\sqrt{2/\pi}$ such that $\mathbb{E}[V_{\mathrm{hub}}] = V_{\mathrm{ave}}$.

The longitudinal turbulence standard deviation σ and the mean longitudinal turbulence intensity $\bar{I}$ follow the NTM, i.e. $\sigma = I_{\text{ref}}(0.75V_{\text{hub}} + b)$, with $b = 5.6\,\text{m/s}$ and $\bar{I} = \sigma/V_{\text{hub}}$.

Although not required by the IEC standard, we assume the turbulence intensity is log normally distributed with mean $\bar{I}$ and standard deviation $\sigma_I = \bar{I}/10$. The resulting PDF then becomes:

$$\rho(I \mid V_{\text{hub}}) = \frac{1}{Is\sqrt{2\pi}} \exp\left[-\frac{(\log I - m)^2}{2s^2}\right], \tag{4.2}$$

$$\text{with } m = \log(\bar{I}^2/\sqrt{\sigma_I^2 + \bar{I}^2}) \text{ and } s = \sqrt{\log(\sigma_I^2/\bar{I}^2 + 1)}. \tag{4.3}$$

The Leja nodes for the turbulence intensity are unweighted Leja nodes on $[0, 0.5]$.

The lateral I_y and vertical I_z turbulence intensity become as follows: $I_y = 0.8I$ and $I_z = 0.5I$. The wind direction is assumed to be distributed uniformly between $-8°$ and $8°$, where $0°$ is wind from north (see Figure 4, where north is indicated). A non-zero degree means that the turbine is yawed. The PDF therefore becomes $\rho(\theta_{\text{dir}}) = 1/16$ if $-8° \leq \theta_{\text{dir}} \leq 8°$, and $\rho(\theta_{\text{dir}}) = 0$ otherwise.

In conclusion, the parameter V_{hub} is distributed according to a Rayleigh distribution and the parameter I is distributed according to a log normal distribution and depends on V_{hub}. The wind direction is distributed uniformly between $-8°$ and $8°$, independently of V_{hub} and I_{ref}.

4.2. Sea conditions

There is no prescribed distribution for the sea conditions, as the conditions vary highly depending on the depth and the currents of the location of the site. In the most simple case, which will be used here, it consists of only the prescription of a joint PDF of the significant wave height H_s, peak spectral period T_p, and V_{hub}. The distribution of V_{hub} is already prescribed, so the resulting joint distribution is denoted by $\rho(H_s, T_p \mid V_{\text{hub}})$. The wave spectrum under consideration is the Jonswap spectrum. The wave direction is kept constant at $0°$ (from north).

It is not uncommon to assume that H_s depends only on V_{hub} by means of a polynomial of degree 2 and to assume that the peak spectral period scales with $\sqrt{H_s}$ [19]. To this end, the distribution is rewritten by using $\rho(H_s, T_p \mid V_{\text{hub}}) \propto \rho(H_s \mid V_{\text{hub}})\rho(T_p \mid V_{\text{hub}}, H_s)$ and then both $\rho(H_s \mid V_{\text{hub}})$ and $\rho(T_p \mid V_{\text{hub}}, H_s)$ are truncated Gaussian distributed, to ensure that there are no regions containing non-physical values with positive probability. The following formulas based on well-known rules of thumb are used for the mean and standard deviation [20]:

$$\bar{H}_s(V_{\text{hub}}) = aV_{\text{hub}}^2 + bV_{\text{hub}} + c, \text{ with } a = 3.45 \times 10^{-3}, b = 4.46 \times 10^{-2}, c = 6.44 \times 10^{-1}, \tag{4.4}$$

$$\sigma_{H_s} = V_{\text{hub}}/50, \tag{4.5}$$

$$\bar{T}_p(V_{\text{hub}}) = 3.6\sqrt{H_s} + 1.5, \tag{4.6}$$

$$\sigma_{T_p} = 0.1. \tag{4.7}$$

The truncation is such that the distribution is defined on $\mu \pm 2\sigma$, i.e. on a two times standard deviation interval around the mean.

4.3. Results

Following the notation from Section 2, the uncertain parameters and their distributions are denoted as follows:

$$x = (V_{\text{hub}}, I, \theta_{\text{dir}}, H_s, T_p)^{\text{T}}, \tag{4.8}$$

and the full PDF can be written as

$$\rho(x) = \rho(V_{\text{hub}}, I, \theta_{\text{dir}}, H_s, T_p) \propto \rho(V_{\text{hub}})\rho(I \mid V_{\text{hub}})\rho(\theta_{\text{dir}})\rho(H_s \mid V_{\text{hub}})\rho(T_p \mid V_{\text{hub}}, H_s). \tag{4.9}$$

Table 2: Environmental parameters used for the load analysis. Uncertain parameters are depicted in *italic*.

Annual average wind speed, V_{ave}	$0.2V_{\text{ref}} = 10\,\text{m/s}$
Turbulence intensity, I_{ref}	0.16
Mean wind speed at hub height, V_{hub}	*Rayleigh distributed*
Longitudinal turbulence intensity, I	*Gaussian distributed depending on* V_{hub}
Wind direction, θ_{dir}	*Uniformly distributed*
Significant wave height, H_s	*Truncated Gaussian distributed depending on* V_{hub}
Peak spectral period, T_p	*Truncated Gaussian distributed depending on* H_s, V_{hub}

Table 3: Mean and standard deviation of the forces acting on the hub and halfway the blades and the moment acting on the jacket base.

	Hub F_x	Jacket base M_z	Blade F_x
μ	$6.43 \times 10^5\,\text{N}$	$2.01 \times 10^6\,\text{N m}$	$1.86 \times 10^5\,\text{N}$
			$1.77 \times 10^5\,\text{N}$
			$2.20 \times 10^5\,\text{N}$
σ	$4.40 \times 10^5\,\text{N}$	$9.25 \times 10^5\,\text{N m}$	$6.40 \times 10^4\,\text{N}$
			$7.17 \times 10^4\,\text{N}$
			$7.26 \times 10^4\,\text{N}$

For the purpose of this article, the ultimate loads on the jacket base, hub, and blades are considered, even though BLADED readily provides the loads on other components as well. In total, 100 Leja nodes are used to construct the interpolant using $\zeta = 1/3$, chosen such that the key features of $\rho(x)$ are carried over. For each node, the simulation is repeated 5 times (the usual number of seeds in a bin) and averaged, as the turbulent wind field still contains a random component. The maximum error between the interpolant generated with 98, 99, and 100 Leja nodes respectively is smaller than the sampling error of the Monte Carlo approach that is used to post process the interpolant (using 10^7 samples), so this number of nodes can be assumed to yield an accurate surrogate.

The mean and standard deviation of the force on the hub, the moment of the jacket base (facing south-west, see Figure 4), and the forces on the blades are provided in Table 3. The respective distributions of these parameters are presented in Figure 5 and 6. The jacket base moment is determined with respect to the y-axis in Figure 4 (i.e. the fore-aft moment). These distributions were determined by approximating the histogram using Gaussian densities, resulting in small positive probability for non-physical negative values.

The force acting on the hub of the turbine and the jacket base moment are expected to be positive very often, due to the wind coming from north. This is visible in both densities and in the mean and standard deviation of this force.

The individual forces acting on the three blades have a similar structure, but do differ because a simulation of only 10 minutes is considered (so each blades has a slightly different path through the random wind field). The PDFs describe that the forces are mostly positive, which is physically reasonable as the wind comes from north.

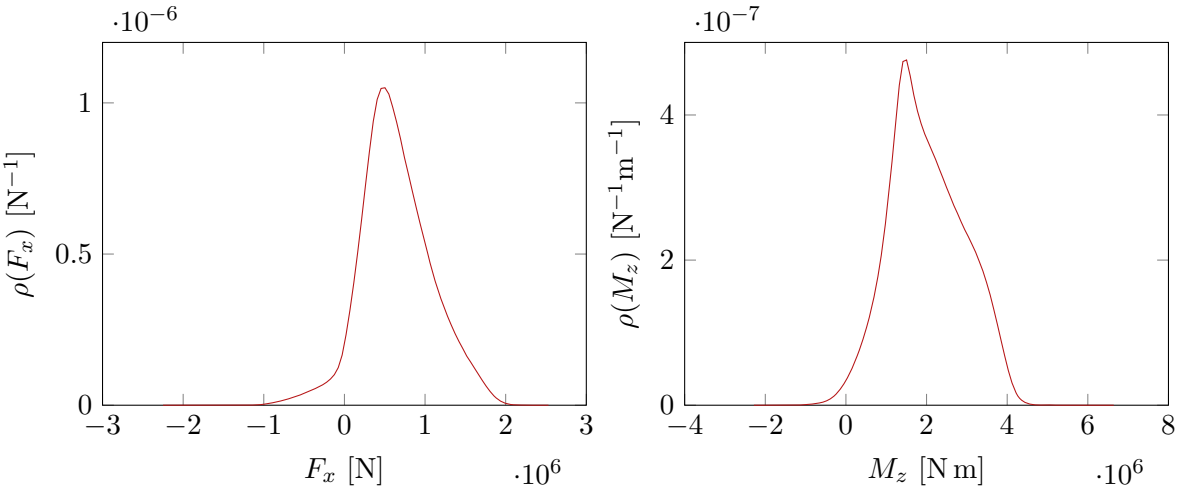

(a) Force on hub **(b)** Moment on jacket base

Figure 5: Probability density functions of the forces acting on the turbine.

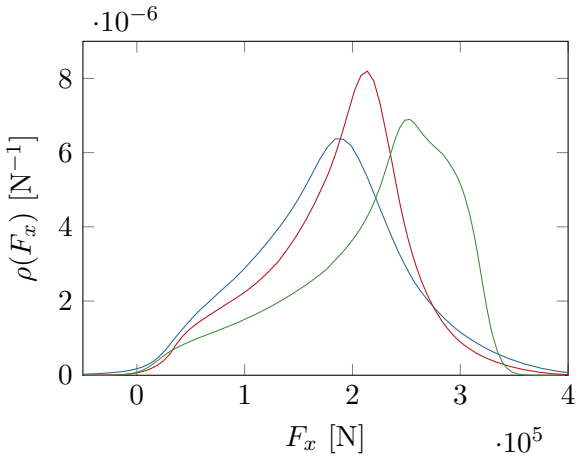

Figure 6: Probability density function of the forces acting the three blades, determined halfway the blades.

5. Conclusions & Future work

In this work the ultimate loads on a wind turbine are determined using uncertain environmental conditions and a polynomial surrogate model. The uncertain parameters are chosen to follow the IEC standard as much as possible.

The results demonstrate that the polynomial interpolant has the potential to be an accurate approach to determine the ultimate loads on various components of the wind turbine. The magnitudes of the quantities are correct, positive quantities are correctly predicted to be positive, and the surrogate is converged correctly. However, the required post processing techniques from the standard are not (yet) incorporated the mathematical framework set out in this article.

The uncertain parameters chosen in this work are not chosen according to specific site conditions, which is the most realistic scenario. Using measurement data, the distributions can be assessed more realistically. This requires additional work on the construction of input distributions incorporating this data. Moreover, if such site conditions are specified, an extensive

comparison can be made with the conventional approach for assessing design load cases.

Acknowledgments
This research is part of the Dutch EUROS program, which is supported by NWO domain Applied and Engineering Sciences and partly funded by the Dutch Ministry of Economic Affairs.

References

[1] IEC 2009 Wind turbines – part 3: Design requirements for offshore wind turbines Tech. Rep. 61400-3 Ed. 1 International Electrotechnical Commission

[2] Burton T, Sharpe D, Jenkins N and Bossanyi E 2001 *Wind Energy Handbook* (Wiley-Blackwell)

[3] Freudenreich K and Argyriadis K 2008 *Wind Energy* **11** 589–600 ISSN 1099-1824

[4] Agarwal P and Manuel L 2008 *Wind Energy* **11** 673–684 ISSN 1099-1824

[5] Ragan P and Manuel L 2007 *45th AIAA Aerospace Sciences Meeting and Exhibit*

[6] Xiu D 2010 *Numerical Methods for Stochastic Computations* (Princeton University Press) ISBN 0691142122

[7] van den Bos L M M and Sanderse B 2017 Uncertainty quantification for wind energy applications Tech. Rep. SC-1701 Centrum Wiskunde & Informatica URL `https://ir.cwi.nl/pub/26650/`

[8] Murcia J P, Réthoré P E, Natarajan A and Sørensen J D 2015 *Journal of Physics: Conference Series* **625** 012030

[9] Petrone G, de Nicola C, Quagliarella D, Witteveen J and Iaccarino G 2011 Wind turbine performance analysis under uncertainty *49th AIAA Aerospace Sciences Meeting including the New Horizons Forum and Aerospace Exposition* (American Institute of Aeronautics and Astronautics (AIAA))

[10] Padrón A S, Thomas J, Stanley A P J, Alonso J J and Ning A 2018 *Wind Energy Science Discussions* 1–30 ISSN 2366-7621

[11] Saranyasoontorn K and Manuel L 2008 *Journal of Wind Engineering and Industrial Aerodynamics* **96** 503–523

[12] Graf P, Dykes K, Damiani R, Jonkman J and Veers P 2017 *Wind Energy Science Discussions* 1–16

[13] Graf P, Damiani R, Dykes K and Jonkman J M 2017 Advances in the assessment of wind turbine operating extreme loads via more efficient calculation approaches *35th Wind Energy Symposium* (American Institute of Aeronautics and Astronautics)

[14] Jonkman J, Butterfield S, Musial W and Scott G 2009 Definition of a 5-MW reference wind turbine for offshore system development Tech. Rep. NREL/TP-500-38060 National Renewable Energy Laboratory

[15] Berrut J P and Trefethen L N 2004 *SIAM Review* **46** 501–517

[16] Leja F 1957 *Annales Polonici Mathematici* **4** 8–13 URL `http://eudml.org/doc/208291`

[17] van den Bos L M M, Sanderse B, Bierbooms W A A M and van Bussel G J W 2018 *ArXiv 1802.02035v1* (*Preprint* `1802.02035v1`) URL `https://arxiv.org/abs/1802.02035`

[18] IEC 2005 Wind turbines – part 1: Design requirements Tech. Rep. 61400-1 Ed. 3 International Electrotechnical Commission

[19] Holthuijsen L H 2007 *Waves in Oceanic and Coastal Waters* (Cambridge University Press (CUP))

[20] Schiereck G J 2017 *Introduction to Bed, Bank and Shore Protection* (CRC Press) ISBN 9781138433977